Scientia Iranica A (2022) 29(6), 2773–2788

Sharif University of Technology
**Scientia Iranica**
*Transactions A: Civil Engineering*
http://scientiairanica.sharif.edu

# Estimation of earthquake frequency content and its effect on dynamic analysis using continuous and discrete wavelet transform

**N. Majidi[a,*], A. Heidari[b], A. Fatehi[b], and H. Heidarzadeh[b]**

a. *Department of Civil Engineering, University of Isfahan, Isfahan, Iran.*
b. *Department of Civil Engineering, Shahrekord University, Chaharmahal and Bakhtiari, Iran.*

Received 14 August 2019; received in revised form 25 February 2021; accepted 10 January 2022

**KEYWORDS**
Wavelet transform;
Frequency content;
Fourier spectrum;
Earthquake.

**Abstract.** Wavelet transform is one of the mathematical concepts for studying the frequency content of waves. It can be divided into two groups, continuous and discrete. In general, the continuous wavelet transform is used to examine the time-frequency relationship, whereas the discrete wavelet transform is used for filtering and noise reduction in waves. In this paper, for the first time, the combination of these two concepts is used for the earthquake acceleration wave. For this purpose, eight earthquakes from four different locations in the world have been selected. Initially, each earthquake is filtered up to 5 stages using a discrete wavelet transform. At each stage of the filter, two waves of approximations and details are obtained. Due to the close approximation of the frequency content of the wave to the original earthquake, the approximate wave is used for subsequent calculations. The Fourier spectrum and the diagram of five of the dominant frequency of the earthquake are plotted in the next step. Also, using the continuous wavelet transform, the time-frequency curves of the main earthquakes and the time-frequency curves of the wave obtained from the discrete wavelet transform are investigated. The goal was to find the best stage of a discrete wavelet filter based on frequency content to reduce computations by more than 80%. The time of the strong ground motion, the structural response of a single degree of freedom, and the dynamical response of the timing of the structure of a degree of freedom are all investigated in the following step. By examining the above parameters, the best-performing wavelet transformation step is inferred.



## 1. Introduction

One of the important issues in earthquake engineering is the correction of waves recorded by acceleration [1]. The recorded acceleration signals are noise-free for a number of reasons. However, the noise cannot be extracted from these signals; therefore, the recorded earthquake wave must be corrected. Currently, the signal is corrected in a conventional way by applying the filter. The conventional and common method for making such an amendment is to use upstream and downstream filters. Earthquake recording is mostly done using seismographs and accelerators [2–5]. Seismographs are very sensitive devices that can record extremely poor earth movements caused by earthquake events with high precision. Data from seismic devices cannot be directly used in earthquake engineering, since they cannot record strong earthquakes in close proximity to earthquake centers, because at

*. *Corresponding author.*
*E-mail addresses: noorollahmajidi1373@gmail.com (N. Majidi); aliheidari1@yahoo.com (A. Heidari); alireza.fatehi3469@gmail.com (A. Fatehi); heidarzadeh@ut.ac.ir (H. Heidarzadeh)*

doi: 10.24200/sci.2022.54226.3662

near distances to earthquake centers, these devices are often saturated and cannot be used for optimal recording of strong ground movements. Parameters reported by seismic stations usually include spatial and temporal coordinates, magnitude, and depth of the earthquake [6–10].

Scaling of acceleration is an important topic in earthquake engineering and structural engineering. The common goal of all studies in the field of scaling down is to reduce the dispersion of the results of dynamic analysis of the timeliness and reliability of the instrumental responses. The selected accelerator map is scaled to fit the desired design. The first studies in this field were used to scale up the maximum acceleration, speed, and displacement in acceleration maps. There are several methods for scaling the earthquake acceleration, one of them is the use of peak ground acceleration [11]. In this paper, the Maximum Earthquake Acceleration method is used to scale up the waves from the discrete and continuous wavelet transform.

Generally, earthquake waves form a set of simpler waves with different frequencies and amplitudes. The frequency of an earthquake indicates that the amplitude of these waves has expanded at different frequencies [12–15]. One of the methods for examining the frequency content is the Fourier spectrum. In this paper, the Fourier spectrum was used to study the frequency content of different waves.

The spectral analysis is performed using a curve of the structure response spectrum with a single degree of freedom. A seismic response curve, also known as a seismic response spectrum, is a curve with two axes, one horizontal and one vertical, one representing the structure's period or frequency and the other representing acceleration, pseudo-acceleration, velocity, pseudo-velocity, or displacement [16–22]. The spectral curve of a specific earthquake is derived from the analysis of structures of a single degree of freedom with different natural frequencies. Therefore, the earthquake spectral curve is one of the parameters that is affected by the frequency of the earthquake. Thus, the displacement response spectrum of the wavelet filter is compared to the displacement response spectrum of the earthquake in this research to assess the competency of the suggested approach.

An earthquake's predominant energy includes the duration of a strong ground motion. Several methods have been proposed to calculate the strong ground duration of acceleration. The total amount of time between the acceleration of the Arias, which is usually between 5 and 95% of the Arias intensity, is a significant time. In this method, Arias intensity is measured in percentages, and time is measured in seconds. An effective period is defined as the duration of an earthquake where more than 90% of the total seismic energy exists. This time is in the range of 5% to 95% of the Arias scale of the earthquake. The uniform duration is the sum of the times when the earth acceleration exceeds a given threshold, which is commonly 5% of the maximum earthquake acceleration. Selective time is the interval between the first and last time the acceleration of the earth's motion exceeds a given threshold. The maximum acceleration value is usually 5% [23,24]. In this study, a long period of time is utilized to examine strong ground motion, which is a frequent practice among engineers.

From a mathematical point of view, the conversion into a wave provides more information about the crude wave. The earthquake wave is an unstable wave because its frequencies do not occur throughout the wave's duration and vary at different times. In their study, researchers employed the wavelet transform as a time-frequency display to determine modal parameters such as natural frequencies, damping ratios, and mold shapes of a vibrating system in the dynamics of structures and earthquake engineering. They investigated the precision of their method using a numerical example to measure the vibration of a tower by wind [25]. Then, using a discrete wavelet transform, they proposed a method to improve earthquake movements. The results showed that earthquakes with a similar response spectrum can have different energy and damage potential [26]. Wavelet transform was also used for earthquake movement analysis, and the correlations between wavelet coefficients and input energy were determined by wavelet analysis. Using these principles, they examined the time-frequency features of the movements [27].

Then, the strong ground motion parameters were calculated using wavelet transform and earthquake acceleration analysis. The results showed that with the use of a wavelet transform, the parameters of the powerful earth movement could be estimated with a negligible error [28].

Some studies examined structural damage. Damage to structures can be investigated using wavelet transform. The results of various studies show the efficiency of the wavelet in this field [29,30].

Using discrete wavelet theory, Heidari and Majidi reduced the computational effort for seismic displacement and seismic velocity curves by more than 93%. They showed that by using the Haar wavelet function, they were able to reduce the calculation error to less than 5% [31]. Using discrete wavelet theory, researchers were able to analyze the association between earthquake frequencies and the natural frequency of structures in another study. In this study, they used a wavelet transform method as an alternative to modal analysis [32].

In this research, for the first time, discrete and continuous wavelet transforms are used simultaneously

to study the frequency content of earthquakes. In time history analysis, spectrum analysis, frequency content, time-frequency analysis, and a strong ground motion, a technique to reduce calculations by over 80% is described in this study. For this purpose, wavelet transforms, vibration equations, response spectrum, February spectrum, and strong ground motion time are used. To do so, each wave of various earthquakes must first be filtered using a discrete wavelet transform with up to five stages. At each stage of the filter, two waves of approximations and details are obtained. Given that the wave of details contains low-energy waves, it can be said that the frequency content of the approximate wave is closer to the original earthquake. This is why the approximate wave is used as the main earthquake substitute. By using this method in each stage of wavelet decomposition, the number of earthquake records is reduced to half of the previous stage. As a result, we can say that the number of computations and the time it takes to complete them has been cut in half. In the next step, the acceleration map, the February spectrum, the frequency content, the dynamic response of the structure of a degree of freedom, the time-frequency diagram, the response spectrum, and the strong ground motion of the various waves are investigated. The purpose of these studies is to find the best wavelet filter stage for optimizing computations.

## 2. Wavelet transform

There was a wavelet transform of mother functions and a different scale [33–39]. The mother functions were used in the wavelet continuity conversion and the scale functions were used in the discrete wavelet transform to separate the frequencies. $\psi$ and $\varphi$ denote the mother functions and wavelet scale, respectively. In this paper, the wavelet transform is used discretely and continuously. Therefore, both mathematical principles are discussed below. A wavelet is an alternate, real or imaginary function with a mean of zero and a finite length. Its space is defined as $\psi(t) \in L^2(R)$. The function $\psi(t)$ is called the mother wavelet, and $L^2(R)$ represents the measurable Hilbert space of integrable quadrilateral functions. The function $\psi(t)$ in both the domain and space-frequency is used to create a family of wavelets and is shown as follows:

$$\psi_{u,s}(x) = \frac{1}{\sqrt{s}}\psi\left(\frac{x-u}{s}\right). \tag{1}$$

In this case, real numbers $s$ and $u$ are scale parameters and wavelet transforms. For a signal whose target is a wavelet filter, the coordinate space $f(t) \in L^2(R)$ is considered, in which $t$ specifies the spatial coordinates. The continuous wavelet transform is defined as the inner product between the signal and the wavelet function:

$$Wf(u,s) = f, \qquad \psi_{u,s} = \frac{1}{\sqrt{s}}\int_{-\infty}^{+\infty} f(t)\psi\left(\frac{t-u}{s}\right)dt. \tag{2}$$

In the above equation, $Wf(u,s)$ is called the wavelet coefficient for $\psi_{u,s}(t)$. The integral of the wavelet transform of the previous equation can be written as the following integral:

$$Wf(u,s) = \frac{1}{\sqrt{s}}\int_{-\infty}^{+\infty} f(t)\psi\left(\frac{-(u-t)}{s}\right)dx$$

$$= \frac{1}{\sqrt{s}} f * \psi\left(\frac{-u}{s}\right) = f * \bar{\psi}_s(u), \tag{3}$$

where $\bar{\psi}_s(x)$ is equal to $1/\sqrt{s}\psi(x/s)$.

In this paper, the Haar mother wavelet was used. The mother function of the Haar wavelet as follows:

$$\psi(t) = \begin{cases} 1 & 0 \le t < 0.5 \\ -1 & 0.5 \le t < 1 \\ 0 & \text{otherwise} \end{cases} \tag{4a}$$

and its scale function is as follows:

$$\varphi(t) = \begin{cases} 1 & 0 \le t \le 1 \\ 0 & \text{otherwise} \end{cases} \tag{4b}$$

In the wavelet transform, there are two parameters: scale and transition. The scale parameter in the wavelet is similar to the scale in the maps. The small scale represents the wave's details, while the large scale represents the wave's lack of detail. The scale, like a mathematical function, compresses or expands a wave. The large scale corresponds to the opening of the wave and the small scale makes the wave compress. The low frequency (large scale) corresponds to the general information of the wave and the large frequency corresponds to the details of the wave information. The high frequencies for a long time were unscathed from the wave, while there were low frequencies throughout the wave. In the continuous wavelet transform, the transmission and scale parameters are continuously changed. In fact, the number of computer changes in each step is very small. This makes computing more efficient [40]. Another type of wavelet transform was called wavelet fracture transformation [41] where wavelet transformation, transmission, and scale were considered discrete. The sampling rate of the time curve points can be reduced in accordance with the Nyquist norm at high scales (low frequencies), reducing the number of computations. The Nyquist sampling rate is the minimum rate at which a continuous wave can be reconstructed. Using the lower filters, it is possible to remove the high frequencies from a wave of length (number of points) and obtain the main

wave. Low frequencies can be removed and wave details acquired using the high pass filter. The wave can be divided into two parts with high and low frequencies using the simultaneous effect of these two filters on the wave. In each step, the approaches and wave details are shown with $A_j$ and $D_j$. However, the main wave is obtained from the main wave with the same number of points as the main wave, which doubles the number of wave points, at each stage, using the filters. To overcome this problem, a sample reduction is used [42]. One of the consecutive points is kept and the other is deleted when the sampling is reduced. Therefore, the number of points per wave is approximately half that of the main wave points. After this step, the number of wave points can still be reduced. Because the maximum wave energy is in its approximation and the shape of this part of the wave is more similar to the wave, the filtering operation for this part of the wave is carried out and the wave is converted into two waves. The number of points in each of these waves is about half the number of points. Although from a theoretical point of view, this can be done a number of times, it is needed in dynamic wave analyses that are very similar to the initial wave and the number of points is sufficiently small. In fact, the rapid conversion of the wavelet acts like a filter bank [42,43].

In this method, approximate waves ($A_j$) and detail waves ($D_j$) were obtained from the following relationships [42]:

$$A_j = ap_{j,k} = \sum_n s(n)h_j^*(n-2^jk), \tag{5}$$

$$D_j = de_{j,k} = \sum_n s(n)g_j^*(n-2^jk), \tag{6}$$

where $h_j$ is the low pass filter and $D_j$ is the high pass filter. The $h$ and $g$ filters were calculated from one step to the next using the following relationships [28]:

$$g_1(n) = g(n), \tag{7}$$

$$h_1(n) = h(n), \tag{8}$$

$$g_{j+1}(n) = \sum_k g_j(k)g(n-2k), \tag{9}$$

$$h_{j+1}(n) = \sum_k h_j(k)g(n-2k). \tag{10}$$

These relationships show that this method is similar to the theory of filters and that the rapid wavelet transform corresponds to the filtering of the filter bank. Its inverse is also the same as the combination of the filter bank. The filters used in the wavelet inverse transformation are shown and derived from the following relationships:

$$\tilde{h}_j(n-2^jk) = 2^{-0.5j}\tilde{\psi}(2^{-j}(t-2^jk)), \tag{11}$$

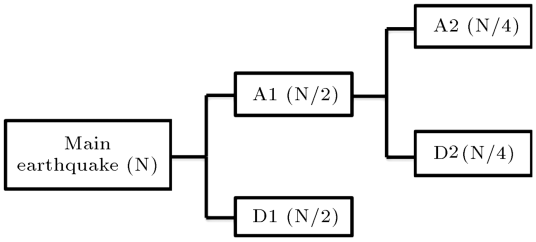


**Figure 1.** Down-sampling method algorithm up to two steps.

$$\tilde{g}_j(n-2^jk) = 2^{-0.5j}\tilde{\varphi}(2^{-j}(t-2^jk)). \tag{12}$$

The values $\psi$ and $\varphi$ are the mother and scale functions. With $\tilde{h}$ and $\tilde{g}$ the values and the main wave can be reconstructed using the following relationship. Figure 1 shows the wavelet transform algorithm:

$$s(n) = \sum_{j=1}^{J}\sum_k ap_{j,k}\tilde{h}_j(n-2^jk) + \sum_{j=1}^{J}\sum_k de_{j,k}\tilde{g}_j(n-2^jk). \tag{13}$$

## 3. Earthquakes used in this article

In this paper, Eight earthquakes have been used to demonstrate the applicability of the proposed technique. Table 1 shows the earthquakes used and their characteristics.

For various earthquakes, the acceleration of the original earthquake and acceleration of the approximation wave wavelet filters are shown in Figure 2. It should be noted that at each stage of the filter the number of earthquake records decreases by half. For example, the A1 to A5 records numbers in the Sarpolzahab earthquake with 19890 records are 9945, 4973, 2486, 1243, and 622, respectively.

As shown in Figure 2, the wavelet filter has good accuracy, which demonstrates the applicability of the proposed technique. With respect to Figure 2, it can be said that with increasing the filter, the approximate wave diverges from the original earthquake. For example, in Figure 2(c) and (h), the A5 wave diverges substantially from the original earthquake.

## 4. Fourier spectrum

Fourier Amplitude Spectrum (FAS) is function that calculate by time by using fast Fourier transform. The Fourier spectrum shows the frequency of earthquake content. The Fourier spectrum represents the dominant frequency of the earthquake. The Fourier spectrum displays the value of wave frequencies.

The desired function $S(t)$ can be shown using a set of sine and cosine functions based on the Fourier transform [44]:

**Table 1.** Selected characteristics of earthquake.

| Earthquake | Country | Date | Earthquake magnitude | Maximum acceleration ($cm/s^2$) | Earthquake time (sec) | Number of records |
|---|---|---|---|---|---|---|
| Sarpolzahab | Iran | 2017-11 | 7.3 | 684.42 | 99.45 | 19890 |
| Friuli | Italy | 1976-05 | 6.5 | 351.30 | 36.32 | 3632 |
| Hollister | USA | 1961-04 | 5.6 | 194.80 | 39.93 | 3993 |
| Northridge | USA | 1994-01 | 6.7 | 568.30 | 39.88 | 3988 |
| Loma_Prieta | USA | 1989-10 | 6.9 | 367.40 | 39.90 | 3990 |
| Imperial_Valley | USA | 1979-10 | 6.5 | 315.20 | 39.48 | 3948 |
| Trinidad | USA | 1983-08 | 3.2 | 193.60 | 21.40 | 2140 |
| Kocaeli | Turkey | 1999-08 | 7.6 | 349.00 | 34.96 | 3496 |

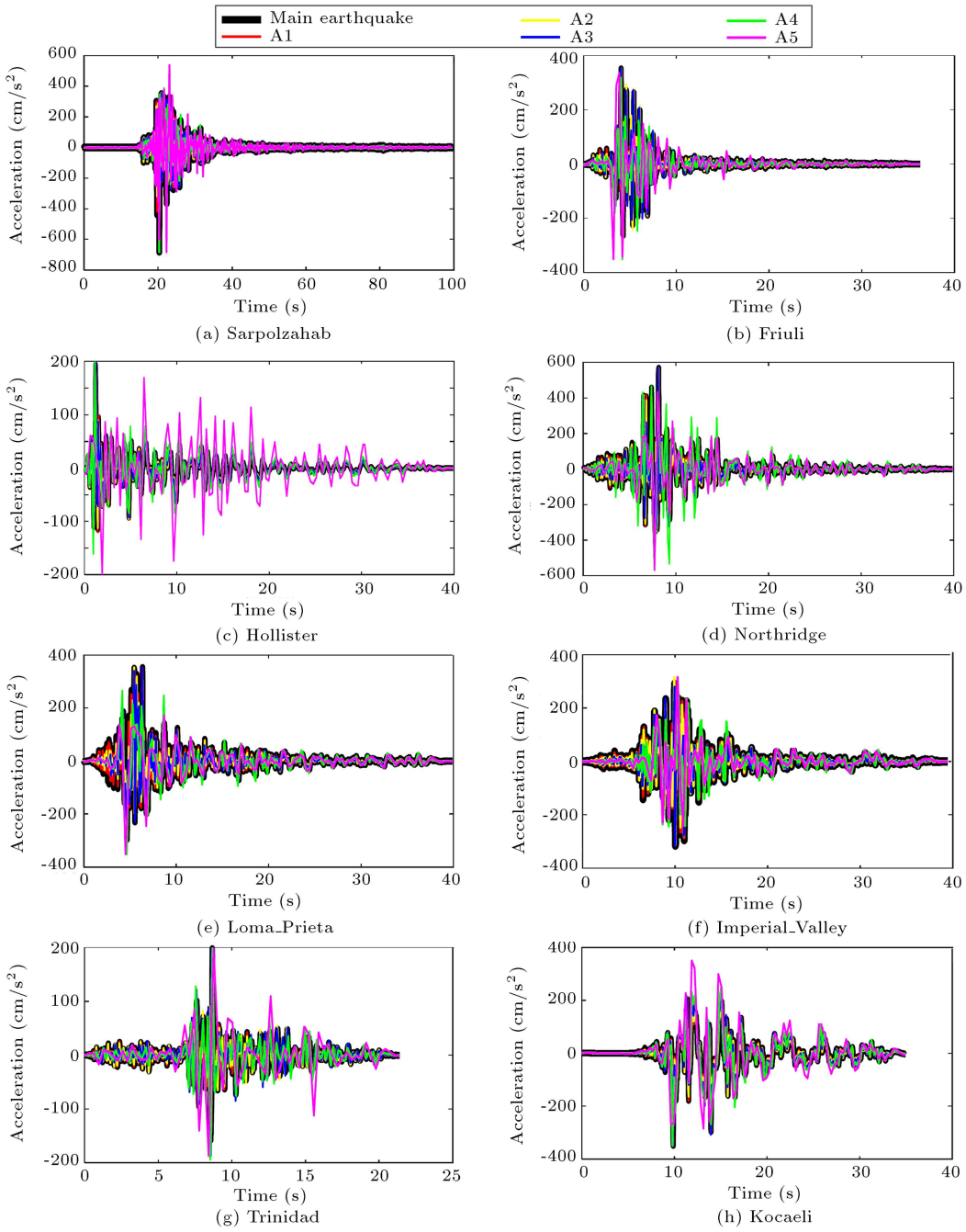


**Figure 2.** Acceleration curve of the main earthquake wave and approximate waves.

$$S(t) = a_0 + a_1 \cos 1\bar{\omega} + a_2 \cos 2\bar{\omega} + \cdots + a_n \cos n\bar{\omega} + b_1 \sin 1\bar{\omega} + b_2 \sin 2\bar{\omega} + \cdots + b_n \sin n\bar{\omega}. \quad (14)$$

The previous function can be rewritten as follows:

$$S(t) = 2\sum_{n=1}^{\infty} \left(a_n \cos\left(n\bar{\omega}t\right) + b_n \sin\left(n\bar{\omega}t\right)\right),$$

$$S(t_j) = \sum_{n=0}^{N-1} C_n e^{-2\pi i(nj/N)},$$

$$j = 0, 1, 2, \cdots, (N-1), \quad (15)$$

$$a_n = \frac{1}{T}\sum_{j=0}^{N-1} S(t_j) \cdot \cos\left(n\bar{\omega}t_j\right)\Delta t, \quad (16)$$

$$b_n = \frac{1}{T}\sum_{j=0}^{N-1} S(t_j) \cdot \sin\left(n\bar{\omega}t_j\right)\Delta t,$$

$$n = 0, 1, 2, \cdots \quad (17)$$

$$C_n = \frac{1}{N}\sum_{j=0}^{N-1} F(t_j) e^{-2\pi(nj/N)},$$

$$N = 0, 1, 2, \cdots, (N-1), \quad (18)$$

$$T = N \cdot \Delta t. \quad (19)$$

In the previous functions, $N$ is the number of records of a discrete function (earthquake), $\Delta t$ is the time step of the earthquake, $T$ is the period of the function, and $\bar{\omega}$ is the frequency. Relation between frequency and period can be written as follows:

$$\bar{\omega} = \frac{2\pi}{T}. \quad (20)$$

$n\bar{\omega}$ can be written as follows:

$$\bar{\omega}_2 = 2\bar{\omega}, \qquad \bar{\omega}_3 = 3\bar{\omega}, \cdots, \qquad \bar{\omega}_n = n\bar{\omega}. \quad (21)$$

FAS can be written as follows:

$$\text{FAS}\left(\bar{\omega}_n\right) = \sqrt{a_n^2 + b_n^2} = \sqrt{Re^2 + \text{Im}^2}. \quad (22)$$

In the previous functions, Re is the real part of $C_n$ and Im is the imaginary part of $C_n$. In Figure 3, the Fourier spectrum of various earthquakes and wavelet filters are plotted.

As shown in Figure 3, the frequency range of the waves from the wavelet filter to the second stage is well approximated. This means that the A2 wave has a good approximation to the original earthquake after reducing 75% of the recordings.

## 5. Dominant frequencies of waves

In this section, five dominant frequencies in various earthquakes and wavelet filters are investigated. The Fourier spectrum of each wave is used to develop the diagram in Figure 4. The purpose of this work is to study the frequency of waves.

Figure 4 shows the frequency number on the horizontal axis and the frequency value on the vertical axis. Figure 4 shows that the first five frequencies of the main earthquakes are similar to those of their wavelet filters. With a reduction of 75% in calculations, the A2 wave can be claimed to be almost effective in all earthquakes. Also, except for Figure 4(a) and (b), it can be said that up to the fourth stage of the filter (wave A4), with 94% reduction in calculations, is predicted with relatively good approximation of the predominant frequencies.

## 6. Time-frequency diagram of various earthquakes

Using the definition of discrete wavelet transform and the continuous wavelet transform, the time-frequency diagram of the waves is plotted. Its worth noting that the goal of these graphs is not to find the dominant frequencies; rather, the goal is to figure out when the dominant frequencies will appear.

A 97% reduction in well-balanced computing predicts the time of dominant of frequencies up to A5 in all earthquakes, as shown in Figure 5. The duration of a higher-energy earthquake is depicted by this curve.

## 7. Time of strong ground motion

In this article, the significant time of the earthquake is investigated. The use of the concept of significant time has been chosen to reduce the earthquake records and also eliminate the noise at the beginning and the end of the earthquake. In Table 2, the start and end time is shown by the strong land motion. As shown in Table 2, wavelet filters can accurately predict the start of strong ground motion in all earthquakes. Furthermore, up to the fifth step filter, the time of the end of the strong ground motion is well predicted in almost all earthquakes (A5).

Using the numbers given in Table 2, the wave associated with strong ground motion is shown in Figure 6.

Figure 6 shows that, with the exception of the A5, the technique used in all phases of the filter is consistent with the original earthquake. Therefore, the A4 wave can be used by reducing 97% of the calculations, instead of the main earthquake.

## 8. Structural response graph of single degree of freedom

In this section, the dynamic response of a structure of a

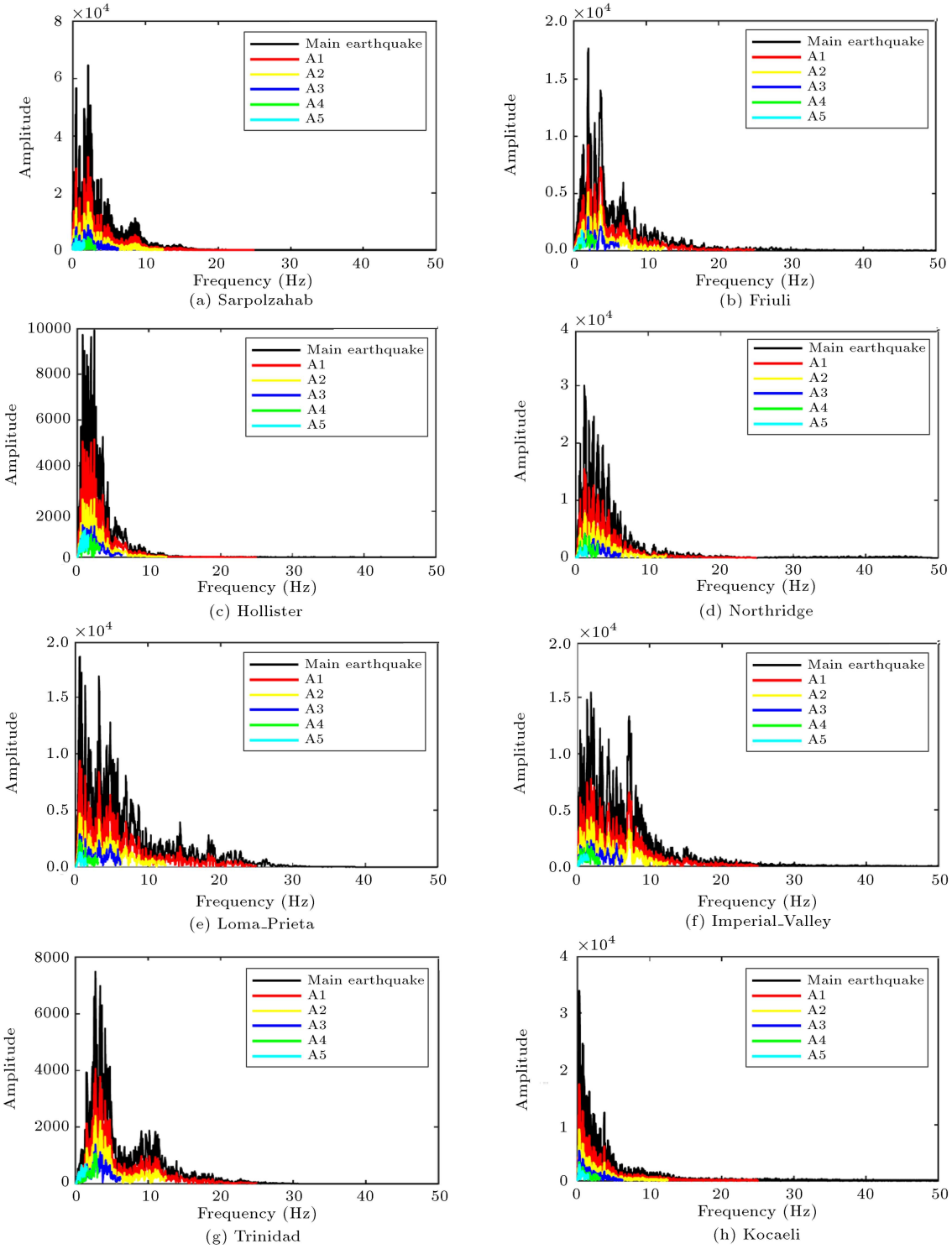


**Figure 3.** Fourier spectrum of various earthquakes and wavelet filters.

degree of freedom with a damping of 5% and a natural frequency of 2 seconds is checked. The purpose of this is to demonstrate the applicability of the proposed method in time history dynamical analysis. Figure 7 shows the dynamic response of the ideal structure for various waves. Figure 7 shows that the A4 wave is the most effective filtering stage in all earthquakes. This wave represents a 96% reduction in calculations that are nearly identical to the original earthquake.

## 9. The earthquake displacement spectrum chart

The displacement spectrum of a structure with a single

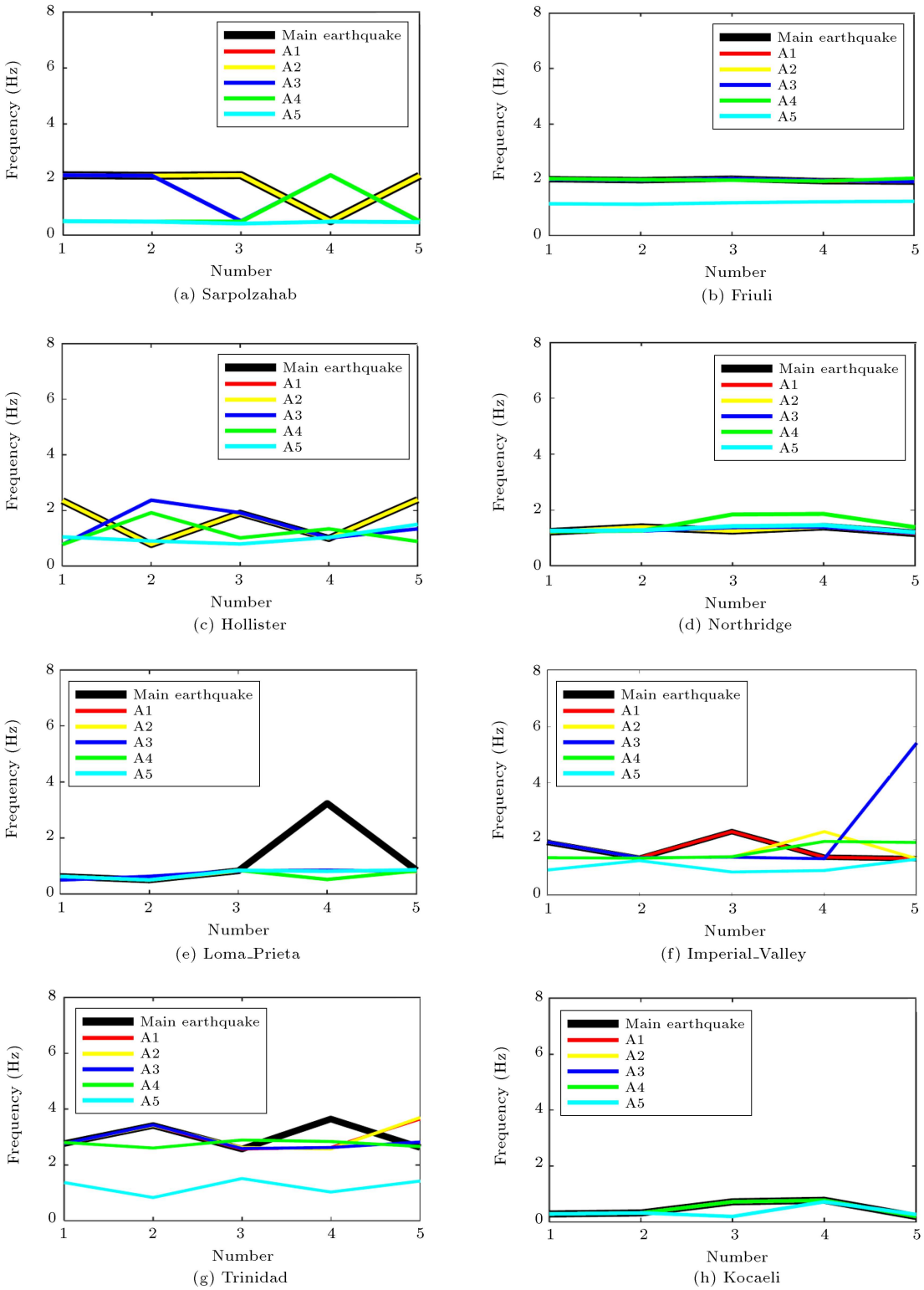


**Figure 4.** Five dominant frequencies of various earthquakes.

degree of freedom and a 5% damping is examined in this section. As shown in Figure 8, the A2 wave in all earthquakes is a good alternative to a major earthquake, with a 75% reduction in calculations.

## 10. Conclusion

In this paper, for the first time, the wavelet transform method was used to reduce computations based on seven different concepts. The concepts were chosen in

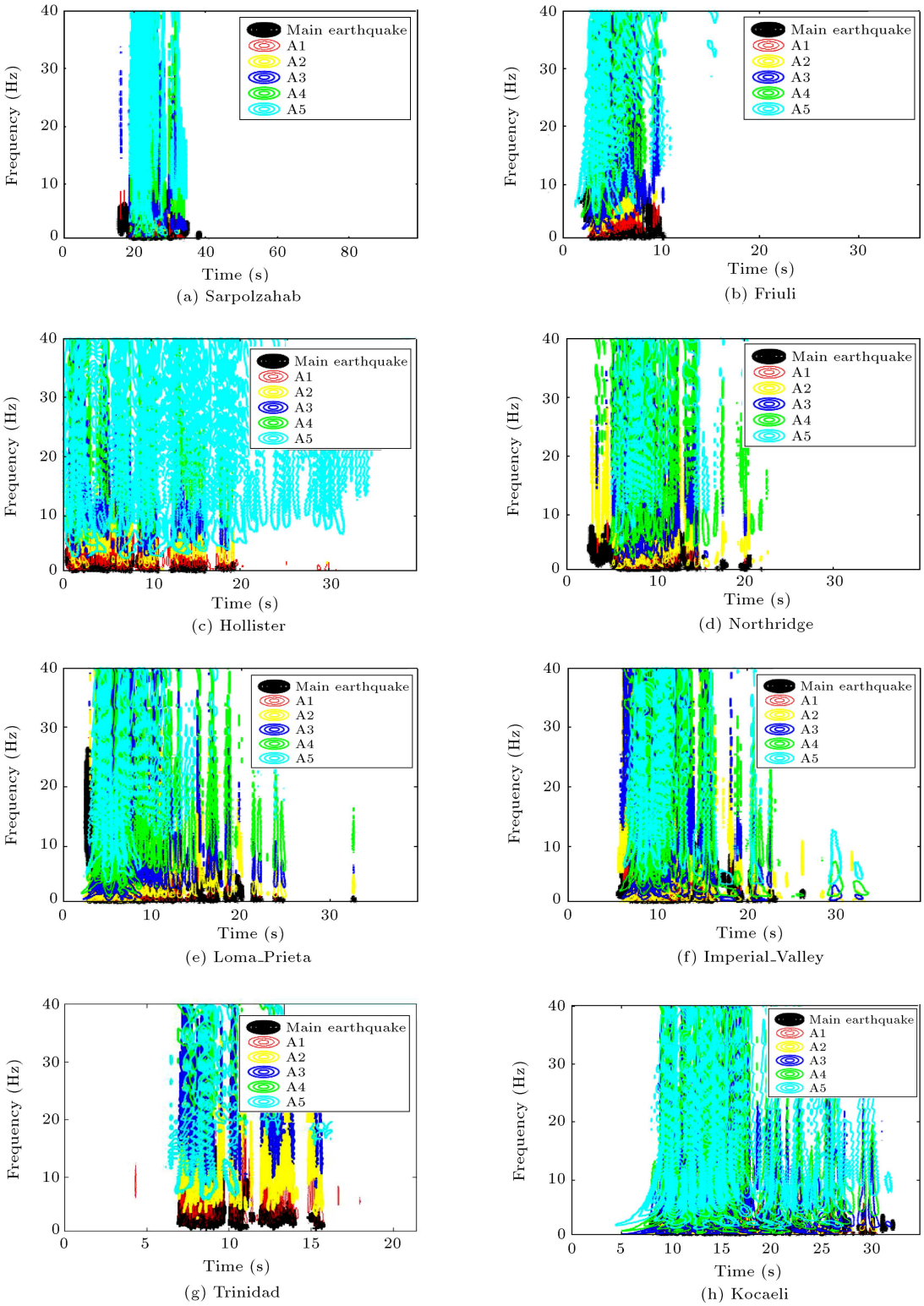


**Figure 5.** Time-frequency diagram of various earthquakes.

such a way that the frequency content of the waves would affect the results. The aim of this study was to investigate the applicability of the wavelet method. Wavelet transform has a good performance in terms of reducing computations, according to the results. To this end, the discrete wavelet filter was applied to earthquakes up to 5 stages. The following conclusions can be drawn from the earthquake study:

1. The wavelet filter can be said to be efficient to stage

**Table 2.** Significant duration of earthquakes.

| Desired earthquake | The wave associated with every earthquake | Significant time (sec) | | |
|---|---|---|---|---|
| | | **Start** | **End** | **Total time** |
| Sarpolzahab | Main wave | 19.58 | 30.41 | 10.83 |
| | A1 | 19.58 | 30.56 | 10.98 |
| | A2 | 19.58 | 30.6 | 11.02 |
| | A3 | 19.6 | 30.72 | 11.12 |
| | A4 | 19.68 | 31.2 | 11.52 |
| | A5 | 19.52 | 31.68 | 12.16 |
| Friuli | Main wave | 3.49 | 7.72 | 4.23 |
| | A1 | 3.46 | 7.92 | 4.46 |
| | A2 | 3.48 | 7.76 | 4.28 |
| | A3 | 3.44 | 7.76 | 4.32 |
| | A4 | 3.36 | 8.16 | 4.8 |
| | A5 | 3.20 | 8.96 | 5.76 |
| Hollister | Main wave | 0.99 | 15.57 | 14.58 |
| | A1 | 0.98 | 15.56 | 14.58 |
| | A2 | 0.96 | 18.00 | 17.04 |
| | A3 | 0.96 | 17.44 | 16.48 |
| | A4 | 0.96 | 18.08 | 17.12 |
| | A5 | 1.92 | 24.96 | 23.04 |
| Northridge | Main wave | 5.37 | 14.45 | 9.08 |
| | A1 | 5.38 | 14.44 | 9.06 |
| | A2 | 5.40 | 14.44 | 9.04 |
| | A3 | 5.60 | 14.4 | 8.8 |
| | A4 | 5.60 | 16.64 | 11.04 |
| | A5 | 6.40 | 19.84 | 13.44 |
| Loma_Prieta | Main wave | 4.00 | 15.31 | 11.31 |
| | A1 | 4.10 | 15.46 | 11.36 |
| | A2 | 4.16 | 15.64 | 11.48 |
| | A3 | 4.16 | 15.92 | 11.76 |
| | A4 | 4.16 | 18.56 | 14.4 |
| | A5 | 3.84 | 16.96 | 13.12 |
| Imperial_Valley | Main wave | 7.08 | 16.00 | 8.92 |
| | A1 | 7.08 | 16.00 | 8.92 |
| | A2 | 7.28 | 16.20 | 8.92 |
| | A3 | 7.76 | 17.04 | 9.28 |
| | A4 | 7.68 | 20.00 | 12.32 |
| | A5 | 8.80 | 20.48 | 11.68 |
| Trinidad | Main wave | 7.13 | 14.93 | 7.80 |
| | A1 | 7.12 | 14.94 | 7.82 |
| | A2 | 7.12 | 14.92 | 7.80 |
| | A3 | 7.12 | 15.12 | 8.00 |
| | A4 | 7.20 | 15.04 | 7.84 |
| | A5 | 7.36 | 15.36 | 8.00 |
| Kocaeli | Main wave | 9.83 | 25.45 | 15.62 |
| | A1 | 9.82 | 25.46 | 15.64 |
| | A2 | 9.84 | 25.48 | 15.64 |
| | A3 | 9.84 | 25.68 | 15.84 |
| | A4 | 9.76 | 25.60 | 15.84 |
| | A5 | 9.60 | 25.60 | 16.00 |

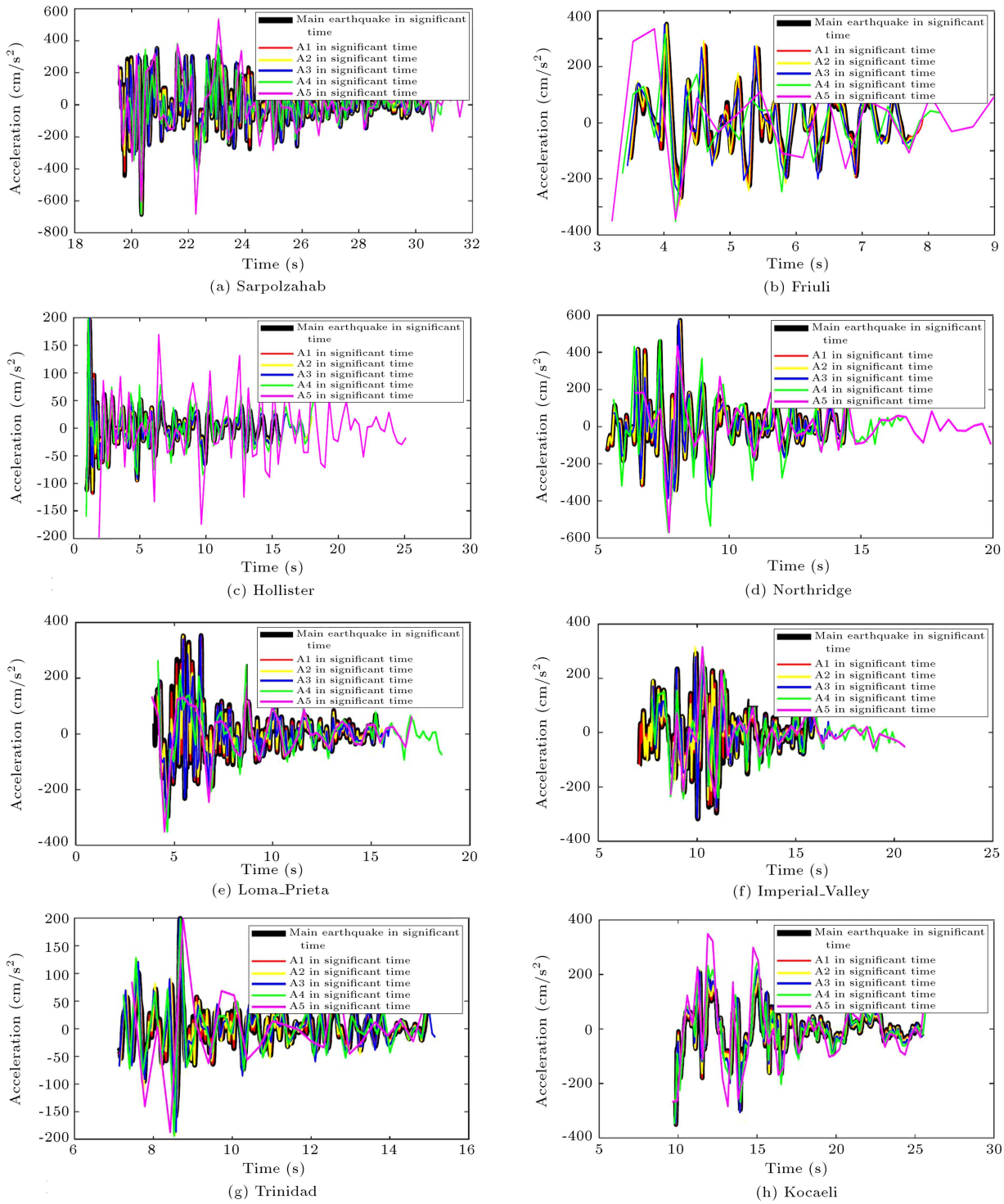


**Figure 6.** Waves of strong ground motion of various earthquakes.

4 based on the acceleration mapping of various earthquakes (A4). Therefore, instead of using the entire earthquake record data, one of their sixteen can be used;

2. The Fourier spectrum of the third level of the wavelet decomposition is close to the main earthquake wave in terms of frequency content;

3. Given the five different earthquake frequencies, it can be seen that an A2 wave is a good option for earthquakes and the calculations are reduced by 75%;

4. The time of the dominant frequencies of all stages of discrete wavelet filters is equal to the time of the dominant frequencies of the earthquake, according

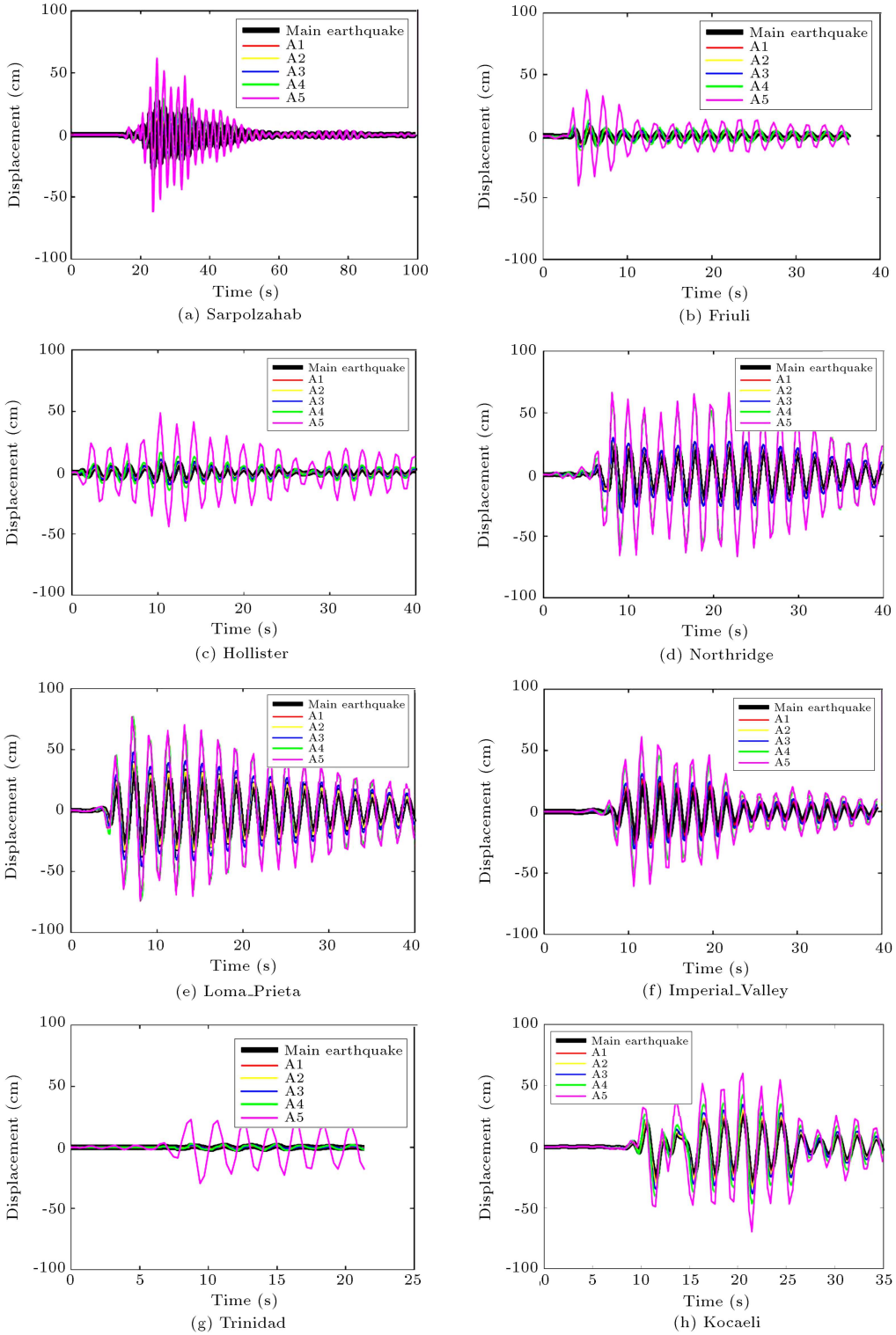


**Figure 7.** Structural response under the impact of various earthquakes.

to the results derived from the time-frequency curve of continuous wavelet transformation for earthquakes. The wavelet filters and seismic energy are interchangeable;

5. According to the part of the wave that corresponds to the time of the earth strong motion, the A4 wave curve corresponds to the original earthquake with a reduction of 97% in the calculation;

6. The response curve of a structure of a single degree of freedom indicates that the response curve

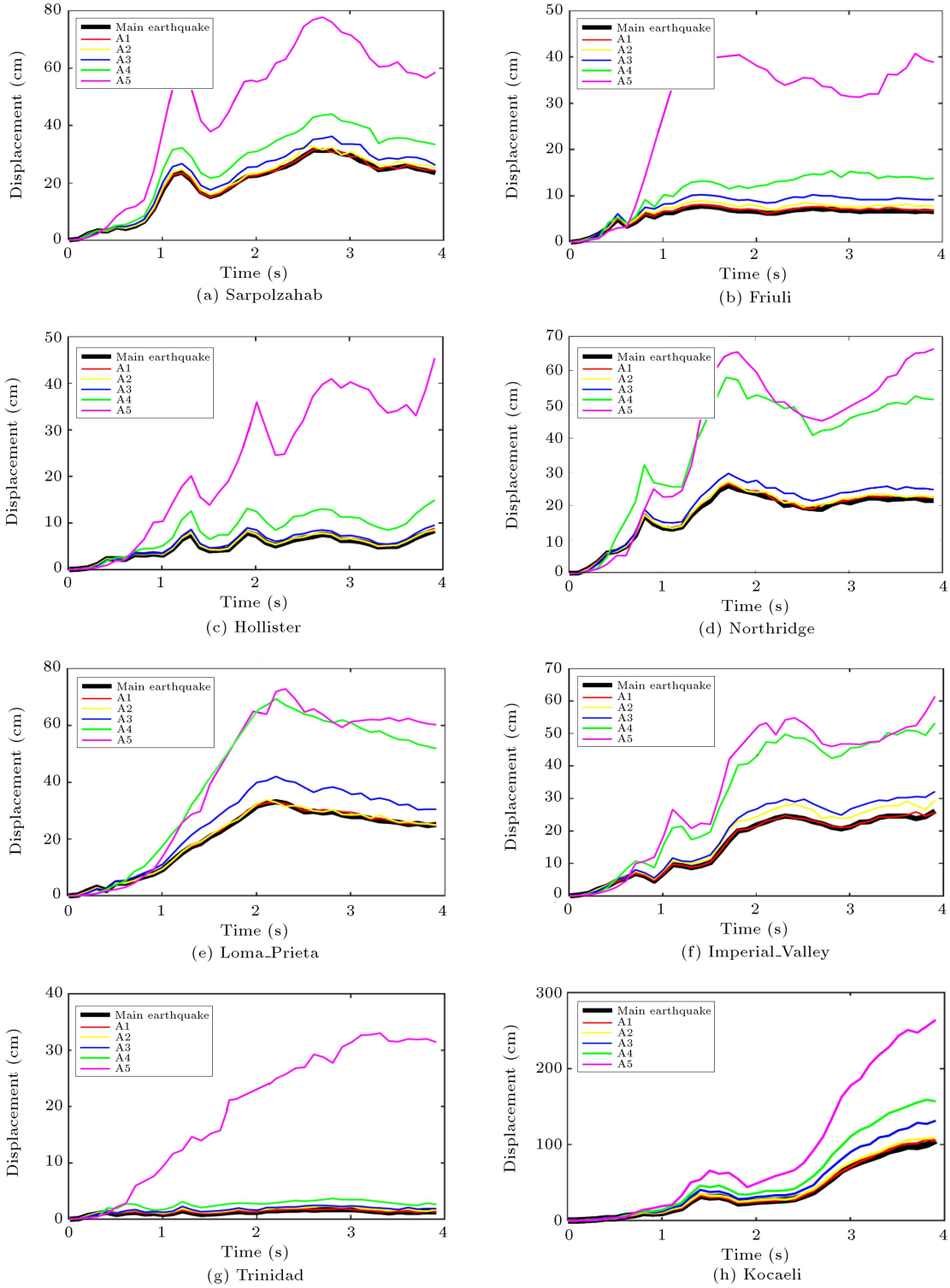


**Figure 8.** Displacement spectrum of various earthquakes.

obtained from the A4 wave with a reduction of 97% of the calculations is well suited to the response curve from the original earthquake;

7. The curve of the displacement spectrum of a structure of a single degree of freedom indicates that the response curve obtained from wave A2 with a decrease of 75% of the calculations is well suited to the original earthquake response curve.

In general, the A2 wave, in all of its seismic dimensions, both in terms of frequency content and energy, is

a good substitute for the main earthquake, allowing calculations to be reduced by up to 75%.

## References


1. Curtis, A., Gerstoft, P., Sato, H., et al. "Seismic interferometry–turning noise into signal", *The Leading Edge*, **25**(9), pp. 1082–1092 (2006).
2. Yaghmaei-Sabegh, S. "Earthquake ground-motion duration estimation using general regression neural network", *Scientia Iranica*, **25**(5), pp. 2425–2439 (2018).
3. Bazmooneh, A. and E. Estekanchi, H. "Determination of target time for endurance time method at different seismic hazard levels", *Scientia Iranica*, **25**(1), pp. 33–49 (2018).
4. Yaghmaei-Sabegh, S., Karami, S., and Hosseini-Moghadam, M. "Selection and scaling of spectrum-compatible ground motion records using hybrid coded genetic algorithms", *Scientia Iranica*, **24**(3), pp. 910–925 (2017).
5. Hassani, N., Ghodrati Amiri, G., Bararnia, M., et al. "Ground motion prediction equation for inelastic spectral displacement in Iran", *Scientia Iranica*, **24**(1), pp. 164–182 (2017).
6. Shahbazi, S., Khatibinia, M., Mansouri, I., et al. "Seismic evaluation of special steel moment frames undergoing near-field earthquakes with forward directivity by considering soil-structure interaction effects", *Scientia Iranica*, **27**(5), pp. 2264–2282 (2020).
7. Dehghan, S.M., Najafgholipour, M.A., and Hooshangi, H. "Seismic behavior of chevron concentrically braced frames with weak beam", *Scientia Iranica*, **27**(1), pp. 41–56 (2020).
8. Saafizaadeh, M. and Bagheripour, M.H. "Evaluation of peak ground acceleration for the city of Kerman through seismic hazard analysis", *Scientia Iranica*, **26**(1), pp. 257–272 (2019).
9. Reitherman, R.K., *Earthquakes and Engineers: an International History*, In, American Society of Civil Engineers (2012).
10. Edwards, B., Zurek, B., van Dedem, E., et al. "Simulations for the development of a ground motion model for induced seismicity in the Groningen gas field, The Netherlands", *Bulletin of Earthquake Engineering*, **17**(8), pp. 4441–4456 (2019).
11. Vassiliou, M.F. and Makris, N. "Estimating time scales and length scales in pulselike earthquake acceleration records with wavelet analysis", *Bulletin of the Seismological Society of America*, **101**(2), pp. 596–618 (2011).
12. Heidari, A. and Raeisi, J. "Investigating the effect of soil type on non-linear response spectrum using wavelet theory", *International Journal of Civil Engineering*, **17**(12), pp. 1909-1918 (2019)
13. Ghaffari, E., E. Estekanchi, H., and Vafai, A. "Application of endurance time method in seismic analysis of bridges", *Scientia Iranica, A*, **27**(4), pp. 1751–1761 (2020).
14. Adhikary, S. and Singh, Y. "Effect of site amplification on inelastic seismic response", *Earthquake Engineering and Engineering Vibration*, **18**(3), pp. 535–554 (2019).
15. Bhargavi, P. and Raghukanth, S.T.G. "Rating damage potential of ground motion records", *Earthquake Engineering and Engineering Vibration*, **18**(2), pp. 233–254 (2019).
16. Chen, B., Wen, Z., and Wang, F. "An improved seismic intensity measure of inelastic spectral acceleration based on MPA to reduce the dispersion in IDA", *International Journal of Civil Engineering*, **16**(1), pp. 57–65 (2018).
17. Park, J.-H. "Seismic hazard level reduction for existing buildings considering remaining building lifespans", *Earthquake Engineering and Engineering Vibration*, **18**(3), pp. 649–661 (2019).
18. Raoufi, R. and Ghafory-Ashtiany, M. "Random vibration of nonlinear structures with stiffness and strength deterioration by modified tail equivalent linearization method", *Earthquake Engineering and Engineering Vibration*, **18**(3), pp. 597–610 (2019).
19. Tasiopoulou, P., Giannakou, A., Drosos, V., et al. "Numerical evaluation of dynamic levee performance due to induced seismicity", *Bulletin of Earthquake Engineering*, **17**(8), pp. 4559–4574 (2019).
20. Zolfaghari, M.R. and Darzi, A. "Ground-motion models for predicting vertical components of PGA, PGV and 5%-damped spectral acceleration (0.01-10 s) in Iran", *Bulletin of Earthquake Engineering*, **17**(7), pp. 3615–3635 (2019).
21. Gholizadeh, S. "Performance-based optimum seismic design of steel structures by a modified firefly algorithm and a new neural network", *Advances in Engineering Software*, **81**, pp. 50–65 (2015).
22. Fakharifar, M., Chen, G., Sneed, L., et al. "Seismic performance of post-mainshock FRP/steel repaired RC bridge columns subjected to aftershocks", *Composites Part B: Engineering*, **72**, pp. 183–198 (2015).
23. Bommer, J.J. and Martinez-Pereira, A. "The effective duration of earthquake strong motion", *Journal of Earthquake Engineering*, **3**(02), pp. 127–172 (1999).
24. Stewart, J.P. and Kramer, S.L., *Geotechnical Aspects of Seismic Hazards*, CRC Press, pp. 123–230 (2004).
25. Lardies, J. and Gouttebroze, S. "Identification of modal parameters using the wavelet transform", *International Journal of Mechanical Sciences*, **44**(11), pp. 2263–2283 (2002).
26. Yazdani, A. and Takada, T. "Wavelet-based generation of energy-and spectrum-compatible earthquake time histories", *Computer-Aided Civil and Infrastructure Engineering*, **24**(8), pp. 623–630 (2009).

27. Iyama, J. and Kuwamura, H. "Application of wavelets to analysis and simulation of earthquake motions", *Earthquake Engineering & Structural Dynamics*, **28**(3), pp. 255–272 (1999).

28. Heidari, A., Raeisi, J., and Kamgar, R. "Application of wavelet theory in determining of strong ground motion parameters", *International Journal of Optimization in Civil Engineering*, **8**, pp. 103–115 (2018).

29. Pnevmatikos, N.G. and Hatzigeorgiou, G.D. "Damage detection of framed structures subjected to earthquake excitation using discrete wavelet analysis", *Bulletin of Earthquake Engineering*, **15**(1), pp. 227–248 (2017).

30. Pnevmatikos, N.G., Blachowski, B., Hatzigeorgiou, G.D., et al. "Wavelet analysis based damage localization in steel frames with bolted connections", *Smart Struct. Syst.*, **18**, pp. 1189–1202 (2016).

31. Heidari, A. and Majidi, N. "Earthquake acceleration analysis using wavelet method", *Earthquake Engineering and Engineering Vibration*, **20**(1), pp. 113–126 (2021).

32. Heidari, A. and Majidi, N. "Investigation of the natural frequency of the structure and earthquake frequencies in the frequency domain using a discrete wavelet (in Persian)", *Sharif Journal of Science and Technology*, **36.2**(2.2), pp. 105–113 (2020). DOI: 10.24200/j30.2019.52464.2472

33. Daubechies, I., *Different Perspectives on Wavelets*, American Mathematical Soc. (2016).

34. Kamgar, R., Dadkhah, M., and Naderpour, H. "Seismic response evaluation of structures using discrete wavelet transform through linear analysis", In *Structures*, Elsevier, pp. 863–882 (2021).

35. Dadkhah, M., Kamgar, R., and Heidarzadeh, H. "Reducing the cost of calculations for incremental dynamic analysis of building structures using the discrete wavelet transform", *Journal of Earthquake Engineering*, **1**(1), pp. 1–26 (2020).

36. Kamgar, R., Majidi, N., and Heidari, A. "Continuous wavelet and Fourier transform methods for the evaluation of the properties of critical excitation", *Amirkabir J. of Civil & Environmental Engineering*, **52**(12), pp. 3125–3144 (2019).

37. Majidi, N. and Heidari, A. "Spectral analysis of structures using wavelet theory and concept of time of strong ground motion", *Amirkabir Journal of Civil & Environmental Engineering*, **52**(7), pp. 1685–1704 (2020) (In Persian).

38. Heidari, A., Raeisi, J., and Pahlavan Sadegh, S. "A new method for calculating earthquake characteristics and nonlinear spectra using wavelet theory", *Journal of Rehabilitation in Civil Engineering*, **8**(1), pp. 50–62 (2020).

39. Nasiri, F., Javdanian, H., and Heidari, A. "Seismic response analysis of embankment dams under decomposed earthquakes", *Geomech. Eng.*, **21**(1), pp. 35–51 (2020).

40. Rioul, O. and Duhamel, P. "Fast algorithms for discrete and continuous wavelet transforms", *IEEE Transactions on Information Theory*, **38**(2), pp. 569–586 (1992).

41. Bose, N.K., *Wavelets and Filter Banks*, Springer, pp. 161–188 (2017).

42. Mallat, S.G. "A theory for multiresolution signal decomposition: the wavelet representation", *IEEE Transactions on Pattern Analysis & Machine Intelligence*, **11**(7), pp. 674–693 (1989).

43. Sundararajan, D., *Discrete Wavelet Transform: A Signal Processing Approach*, John Wiley & Sons (2016).

44. Faroughi, A. and Hosseini, M. "Incremental dynamic analysis of SDOF by using nonlinear earthquake accelerograms based on modified inverse Fourier transform", *Journal of Vibroengineering*, **19**(8), pp. 6170–6182 (2017).

## Biographies

**Noorollah Majidi** is currently a PhD student in Structural Engineering at the University of Isfahan, Iran. He has published more than 20 articles. His field of expertise is around the dynamic analysis and structural optimization. He studies the use of different optimization methods for different types of dampers. He has also done many studies in the field of the design of explosion-proof structures. His main focus is on a variety of methods to reduce computational costs in dynamic analysis. He is now studying the construction of wavelet functions and algorithms for generating approximate waves based on different methods of wave analysis. Majidi is expanding wavelet methods in various structures in order to study in detail the methods of reducing the cost of calculations in dynamic analysis.

**Ali Heidari** obtained his PhD in Civil Engineering from the Shahid Bahonar University of Kerman, Iran. He is a faculty member in the department of civil engineering at Shahrekord University. His teachings include courses in Structural and Earthquake Engineering for students at both bachelor and master levels, including Earthquake Engineering, Structural Analysis, Steel Structures, Strength of Materials, Dynamics of Structures, Bridge Engineering, Theory of Elasticity, and Finite Element Methods. His research interests lie in the area of dynamics of structures, vibration control, earthquake engineering, finite element method,

computational mechanics, seismic design of steel structures, seismic strengthening and seismic improvement, constitutive model, optimization, and tall buildings. He has published more than 100 papers in peer-reviewed and conference proceedings.

**Alireza Fatehi** is currently a PhD student at the Islamic Azad University, Najafabad Branch, Isfahan, Iran. He studies the frequency content of waves and structural engineering. He is also interested in studying concrete technology, structural control, and the functional design of structures. He is now studying increasing dynamic analysis and studying the behavior of structures against a variety of dynamic loads. He is also interested in studying metaheuristic optimization algorithms. Fatehi has also conducted studies in the field of structural control.

**Heisam Heidarzadeh** currently works at Shahrekord University. Heisam does research in Geotechnical Engineering/Civil Engineering. He is a faculty member in the department of civil engineering at Shahrekord University. The main area studied by Heidarzadeh is soil behavior models. He studies the behavior of soil plastics under different loads. However, he also studies dynamic analysis, structural control, and optimization. Heidarzadeh is also interested in various methods of nonlinear analysis.